
Article:
Gan, L.-H., Wu, R., Tian, J.-L. et al. (2017) From C 58 to C 62 and back: Stability, structural similarity, and ring current. Journal of Computational Chemistry, 38 (3). pp. 144-151. ISSN: 0192-8651

https://doi.org/10.1002/jcc.24661

From C_{58} to C_{62} and back: stability, structural similarity and ring current

Li-Hua Gan[1, 2], Rui Wu[2], Jian-Lei Tian[2], Joseph Clarke[1], Christopher Gibson[1] and Patrick W. Fowler[1]

[1]Department of Chemistry, Sheffield University, Sheffield, S3 7HF, UK

[2]School of Chemistry and Chemical Engineering, Southwest University, Chongqing, China 400715

E-mail: ganlh@swu.edu.cn; P.W.Fowler@sheffield.ac.uk

Abstract

An increasing number of observations show that non-classical isomers may play an important role in the formation of fullerenes and their exo- and endo-derivatives. A quantum-mechanical study of all classical isomers of C_{58}, C_{60} and C_{62}, and all non-classical isomers with at most one square or heptagonal face, was carried out. Calculations at the B3LYP/6-31G* level show that the favoured isomers of C_{58}, C_{60} and C_{62} have closely related structures and suggest plausible inter-conversion and growth pathways amongst low-energy isomers. Similarity of the favoured structures is reinforced by comparison of calculated ring currents induced on faces of these polyhedral cages by radial external magnetic fields, implying patterns of magnetic response similar to those of the stable, isolated-pentagon C_{60} molecule.

Introduction

Since the discovery of C_{60} [1], classical fullerenes (carbon cages with hexagonal and pentagonal faces only) have been extensively studied. On the experimental side, some tens of isomers have been isolated and characterized. A striking common feature is that all reported neutral bare fullerene isomers satisfy the isolated-pentagon rule (IPR) [2]. On the theoretical side, all mathematically possible classical isomers from C_{20} to C_{90} and beyond have been studied, and the consensus is that the stable classical isomers typically satisfy a more general rule, i.e., that pentagon adjacencies are minimized [3]. This has also been called the pentagon-adjacency-penalty rule (PAPR) [4, 5]. The focus of studies of classical fullerenes is now moving on to applications [6, 7]. However, an increasing number of experimental and theoretical observations indicate that non-classical isomers play an important role in the formation of metallofullerenes and fullerene derivatives [8-10]. Even for the fullerenes themselves, formation mechanisms are still unclear in terms of the roles of heptagons and/or squares [11]. These remarks suggest that it may be useful to

study the structures and properties of non-classical fullerene isomers. Particularly fruitful may be studies in the region of nuclearity around C_{60}, where IPR fullerenes are mathematically impossible for both C_{58} and C_{62}, and so the intervention of non-classical fullerenes may offer candidates that compete in stability with classical fullerenes [12, 13]. In the present study, we extend the quantum-mechanical study of classical isomers and non-classical isomers of C_{58}, C_{60} and C_{62} that have a single square or heptagonal face and small numbers of pentagon adjacencies. Structures were optimized at the density functional level of theory. It turns out that the most favoured isomers of C_{58}, C_{60} and C_{62} have closely related structures. This similarity motivates discussion of the factors that influence stability and suggests plausible inter-conversion growth pathways amongst low-energy isomers. The relation between favoured structural candidates is further reinforced by comparison of calculated magnetic-response properties, specifically the ring currents induced on faces of the polyhedral cage by a perpendicular external magnetic field.

Computational methods

The strategy adopted here is to generate candidate classical and non-classical fullerene graphs, and then obtain corresponding physically realistic geometric structures for the most promising isomers by using quantum mechanical approaches.

Fullerenes (classical and non-classical) have cubic (trivalent) molecular graphs. A provably complete approach to generation of cubic (trivalent) polyhedral graphs is implemented in the CaGe software [14]. Here we used the CaGe program to generate all fullerenes with (a) one square and ten pentagonal faces; (b) twelve pentagonal faces and (c) one heptagonal and thirteen pentagonal faces, i.e., the classical fullerenes and the minimal departures from them in each direction, for nuclearities 58, 60 and 62. We are using ‘square’ here in a combinational sense to mean a face with four sides, without any implication of special geometry, just as our pentagons, hexagons and heptagons are defined only by their numbers of sides, are not necessarily regular, equilateral or even planar.

Classical fullerenes can be generated by the spiral algorithm [15], which can be extended to non-classical fullerenes. An adapted version of the spiral program was used to construct the same sets of both classical and non-classical isomers and assign them a spiral code and hence a

canonical sequence number. We note that although there are classical and non-classical fullerenes that have no face spirals [16], the algorithm is complete for the sets described here. In-house programs were used to calculate 'topological coordinates' derived from adjacency eigenvectors [15] and invariants related to combinational curvature, such as counts of edge type, and triples types of faces meetings at vertices.

The search was deliberately restricted to fullerenes with at most one 'defect' face: face sizes of less than five impose an evident energy penalty, which is ascribed to strain arising from repulsion between the adjacent bonding electronic pair within the face [17]; sizes greater than six imply the inclusion of extra sub-hexagonal faces according to the Euler theorem. Previous studies have suggested that energies of carbon cages rise rapidly with the numbers of both sub-hexagonal [18, 19] and larger [20] faces.

The numbers of classical isomers are 1205, 1812 and 2385 for 58, 60 and 62 vertices, respectively; the numbers of non-classical isomers with a single square defect are 5647, 7475 and 10323, and with a single heptagon are 22789, 36295 and 56950, respectively. Isomers are labeled as $C_n - x - k$, $C_n^{1h} - x - k$ and $C_n^{1s} - x - k$, where $1h$ and $1s$ denote non-classical fullerenes with a heptagon or square, x (also known as N_{55}) denotes the number of fusion(s) of two pentagons, and k is the position of the isomer in the order of the lexicographically minimum face spirals. This is an extension of the IUPAC nomenclature for classical fullerenes. Structures of isomers with low values of N_{55} were optimized, starting from the topological coordinates, at the semi-empirical PM3 level to give plausible starting structures and then with DFT methods at B3LYP/3-21G and B3LYP/6-31G* levels. All the calculations were carried out with Gaussian 09 [21]. Energetic and structural parameters are listed in Table 1. The optimized structures of the two isomers of lowest energy for each C_n are shown in Figure 1 and Schlegel diagrams are shown in Figure 2. Frequency calculations at the B3LYP/6-31G* level were carried out to check that optimized geometrical structures of the favoured isomers correspond to local minima on the potential hypersurface; asphericity values and pyramidalization angles were calculated based on the optimized structures. Ring-current calculations were also performed at the pseudo-π level [22-24] with the SYSMO program [25] for these 3D structures, as discussed below.

Table 1 Calculated relative energies (ΔE, kcal/mol), asphericities (AS), and HOMO-LUMO gaps (eV) at the B3LYP/6-31G* level, indexed by an IUPAC-style isomer label based on the spiral algorithm.

C_{58}	Δ E	AS	Gap	IUPAC	C_{60}	Δ E	AS	Gap	IUPAC	C_{62}	Δ E	AS	Gap	IUPAC
C_{58}-3-1	0.0	0.06	0.92	1205	C_{60}-0-1	0.0	0.00	2.76	1812	C_{62}-3-3	0.0	0.19	1.29	2378
C_{58}-4-1	12.4	0.31	1.40	1078	C_{60}-2-1	38.9	0.06	1.96	1809	C_{62}-3-2	0.8	0.19	1.12	2377
C_{58}-4-4	13.4	0.07	1.29	1198	C_{60}-3-3	57.9	0.09	2.00	1804	C_{62}-3-1	2.4	0.22	1.27	2194
C_{58}-4-2	15.0	0.11	1.15	1195	C_{60}-3-2	58.3	0.05	2.00	1803	C_{62}-4-16	11.1	0.16	1.66	2182
C_{58}-4-3	15.6	0.16	0.93	1196	C_{60}-3-1	75.2	0.18	0.96	1789	C_{62}-4-21	11.3	0.44	1.49	2336
C_{58}-5-21	29.4	0.21	1.38	1155	C_{60}-4-14	77.2	0.09	1.97	1806	C_{62}-4-17	14.1	0.20	1.39	2184
C_{58}-5-14	30.0	0.30	1.44	1105	C_{60}-4-13	77.2	0.17	1.96	1805	C_{62}-4-1	14.3	0.61	1.25	1914
C_{58}-5-16	30.1	0.37	1.41	1107	C_{60}-4-16	78.5	0.16	1.72	1808	C_{62}-4-8	16.1	0.63	2.08	1997
C_{58}-5-12	31.6	0.27	1.27	1079	C_{60}-4-17	78.9	0.19	1.59	1810	C_{62}-4-20	16.2	0.28	1.52	2277
C_{58}-5-3	34.3	0.52	1.74	898	C_{60}-4-15	80.0	0.13	1.53	1807	C_{62}-4-23	17.7	0.50	1.84	2338
C_{58}^{1s}-2-6	28.6	0.56	2.22	4337	C_{60}^{1s}-2-12	108.9	0.18	1.03	6223	C_{62}^{1s}-0-1	-10.4	0.13	1.84	9620
C_{58}^{1s}-2-8	30.1	0.30	1.57	4464	C_{60}^{1s}-2-14	115.1	0.24	1.34	6792	C_{62}^{1s}-1-1	10.2	0.25	1.86	8255
C_{58}^{1s}-2-4	32.5	0.52	1.92	4329	C_{60}^{1s}-2-11	115.7	0.34	1.04	5897	C_{62}^{1s}-2-34	24.8	0.09	1.24	9899
C_{58}^{1s}-2-5	38.6	0.53	1.96	4332	C_{60}^{1s}-3-169	123.0	0.46	1.56	5772	C_{62}^{1s}-2-35	25.5	0.24	1.98	10323
C_{58}^{1s}-3-88	43.1	0.27	1.96	4713	C_{60}^{1s}-3-162	124.4	0.44	1.56	5688	C_{62}^{1s}-2-23	25.7	0.24	2.07	8256
C_{58}^{1s}-3-89	44.0	0.23	1.67	4715	C_{60}^{1s}-3-161	124.9	0.46	1.67	5687	C_{62}^{1s}-2-33	28.1	0.17	1.57	9618
C_{58}^{1s}-2-7	45.6	0.36	0.84	4379	C_{60}^{1s}-3-189	125.2	0.17	1.60	6216	C_{62}^{1s}-2-32	29.5	0.17	1.74	9611
C_{58}^{1s}-3-86	46.3	0.32	1.56	4644	C_{60}^{1s}-3-190	125.9	0.19	1.39	6219	C_{62}^{1s}-1-2	31.2	0.24	1.03	9117
C_{58}^{1s}-3-57	48.2	0.51	1.58	3790	C_{60}^{1s}-3-188	126.4	0.25	1.48	6214	C_{62}^{1s}-2-21	31.6	0.20	1.98	8157
C_{58}^{1s}-3-79	51.3	0.39	1.64	4463	C_{60}^{1s}-3-142	127.8	0.54	1.68	5262	C_{62}^{1s}-2-20	35.3	0.26	1.64	8156
C_{58}^{1h}-4-1	2.5	0.11	1.55	2003	C_{60}^{1h}-4-1	87.3	0.32	1.37	15855	C_{62}^{1h}-3-1	-13.5	0.12	1.38	4644
C_{58}^{1h}-5-4	10.6	0.12	1.33	2055	C_{60}^{1h}-5-8	89.0	0.17	1.66	6807	C_{62}^{1h}-4-4	-2.0	0.11	1.36	4697
C_{58}^{1h}-5-3	11.0	0.10	1.33	2010	C_{60}^{1h}-4-2	91.2	0.22	1.00	16050	C_{62}^{1h}-4-5	-1.1	0.08	1.25	4718
C_{58}^{1h}-5-1	22.2	0.21	1.71	1902	C_{60}^{1h}-5-1	91.5	0.10	1.25	2942	C_{62}^{1h}-4-3	1.7	0.20	1.62	4564
C_{58}^{1h}-5-2	24.5	0.18	1.43	2001	C_{60}^{1h}-5-7	96.6	0.08	1.20	3142	C_{62}^{1h}-4-1	12.8	0.17	1.79	4118
C_{58}^{1h}-6-31	28.4	0.16	1.51	2052	C_{60}^{1h}-6-114	99.1	0.33	1.42	6791	C_{62}^{1h}-4-12	14.0	0.35	1.42	48087
C_{58}^{1h}-6-30	29.3	0.23	1.64	2051	C_{60}^{1h}-5-33	100.5	0.22	1.29	35540	C_{62}^{1h}-5-67	14.7	0.12	1.35	4747
C_{58}^{1h}-6-23	30.2	0.14	1.32	2011	C_{60}^{1h}-5-21	101.2	0.30	0.05	16044	C_{62}^{1h}-5-68	15.1	0.08	1.44	4736
C_{58}^{1h}-6-27	30.5	0.17	1.52	2026	C_{60}^{1h}-5-6	103.4	0.18	1.15	3097	C_{62}^{1h}-5-70	15.2	0.13	1.33	4753
C_{58}^{1h}-6-4	31.3	0.19	1.24	1910	C_{60}^{1h}-5-31	104.8	0.44	1.63	30364	C_{62}^{1h}-5-69	16.8	0.09	1.32	4737

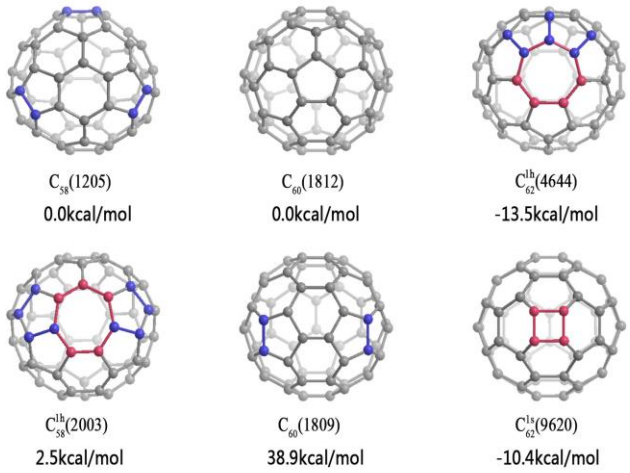

Fig.1. Best isomers of C_{58}, C_{60} and C_{62}, optimized at the B3LYP/6-31G* level, with energies relative to the classical structure of lowest energy (which for C_{62} is isomer 2378).

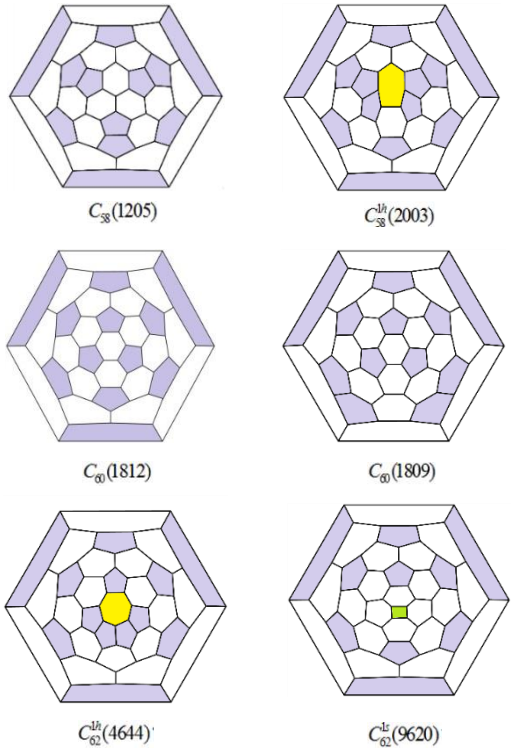

Fig.2. Schlegel diagrams for the lowest energy isomers of C_{58}, C_{60} and C_{62}.

3 Results and Discussion

3.1 DFT results

A striking feature of Table 1 and Figure 1 is that the set of classical fullerenes in this size range does not necessarily include the candidate cage of lowest energy. For C_{58}, the best candidate is classical, although a non-classical isomer lies only 2.5 kcal/mol higher in energy; for C_{60} non-classical isomers are not found within the first ten; for C_{62}, the first four isomers in order of energy are non-classical. The results for the three isomer types are now reviewed in turn.

Classical fullerenes

Classical fullerenes C_n with n = 58, 60, 62 have at least 3, 0, and 3 pentagon adjacencies (counted by N_{55}), respectively. There are 1, 1 and 3 isomers that realize the respective minimum values of N_{55}. Within the classical set, the isomer with lowest energy at the B3LYP/6-31G* level (Table 1) realizes the minimum N_{55} in all three cases. Table 1 indicates a penalty for pentagon adjacency of at least 10 kcal/mol for the classical fullerenes from C_{58} to C_{62}. These results are consistent with previously reported calculations [13, 26]. Within this set, N_{55} can be used as a useful ranking criterion: for C_{58}, all classical isomers with fewer fused pentagons are lower in energy than those with more; for C_{60} and C_{62}, most but not all classical isomers also obey this rule.

Isomers containing a square face

Cages with a single square face and all others pentagonal and hexagonal have $N_{55} \geq 2$ for C_{58} and C_{60}, but a C_{62} cage can achieve $N_{55} = 0$ (isomer C_{62}^{1s}-0-1(9620) has C_{2V} symmetry, and no edges of type 45 or 55).

For C_{58}, the isomer C_{58}^{1s}-2-6(4337) with $N_{55} = 2$ lies 28.56 kcal/mol higher in energy than the best classical isomer $C_{58}-3-1(1205)$ ($N_{55}=3$). All 98 isomers of C_{58} that have a single square face and $N_{55} = 3$ lie at least 46 kcal/mol higher than the best classical isomer with $N_{55} = 3$.

For C_{60}, the most favoured isomer with a square is C_{60}^{1s}-2-12(6223), which lies 108.9 kcal/mol higher in energy than the most favoured classical fullerene C_{60}-0-1(1812), and 70 kcal/mol higher than the unique classical isomer with $N_{55} = 2$, i.e., C_{60}-2-1(1809), but the present results show directly that inclusion of a square in the fullerene framework is intrinsically unfavourable at sizes

around 60. Inclusion of square faces can be favourable for small fullerenes [18, 19], where it can reduce the number of pentagon-pentagon contacts. However, for C_{60}, the cost of inclusion of the square face is evidently not offset by the reduction in N_{55}.

For C_{62}, the most favoured isomer with a square, C_{62}^{1s}-0-1(9620) lies 10.4 kcal/mol lower in energy than the most favoured classical isomer. Nevertheless, all square-containing isomers of C_{62} have energies at least 35.0 kcal/mol higher than for classical isomers with the same number of pentagon adjacencies.

These penalties are compatible with the experimental observation that no square-containing all-carbon fullerene isomer has yet been isolated. Within the one-square class and for each n, isomers of C_n, with higher N_{55} are generally higher in energy than those with lower N_{55}, and hence continue to satisfy the minimum-pentagon-adjacency rule of thumb, with an energy penalty per adjacency of more than 10 kcal/mol.

Isomers containing one heptagonal face

Cages with one face heptagonal and all others pentagonal or hexagonal have $N_{55} \geq 4$ for C_{58} and C_{60} and $N_{55} \geq 3$ for C_{62}. For C_{58}, the isomer of lowest energy in this class is C_{58}^{1h}-4-1(2003) and it lies only 2.5 kcal/mol higher than the best classical fullerene, and lower by 9.9 kcal/mol in energy than the second best classical C_{58}-4-1(1078) with which it shares the value of $N_{55} = 4$. For C_{60}, the best one-heptagon isomer is C_{60}^{1h}-4-1, which lies 87.3 kcal/mol higher than the best classical cage and at least 10.0 kcal/mol higher than the best classical isomers with $N_{55} = 4$. For C_{62}, however, the most favoured heptagon-containing isomer is C_{62}^{1h}-3-1(4644), 13.5 kcal/mol lower in energy than the most favoured classical C_{62} fullerene. Two further one-heptagon isomers $C_{62}^{1h}-4-4$ and $C_{62}^{1h}-4-5$ with $N_{55} = 4$, are also of lower energy than the best classical isomer. Within the one-heptagon subclass, energy generally rises with N_{55}. The one-heptagon class of non-classical fullerenes has, therefore, furnished the C_{62}.candidate of lowest energy.

3.2 Discussion

Minimum-pentagon-adjacency rule

As noted above, minimization of N_{55} within the three subclasses offers a useful guide to relative stability. However, the relative energies between groups do not simply follow this rule. Schemes in which numbers of edges of all combinational types are assigned energy costs or benefits suggest a balancing of factors. Increases in N_{44}, N_{55} and N_{77} all bring substantial costs. The mixed edge type N_{57} is always energetically favourable; edges of this type are associated with an azulenoid fragment, which gives local planarity and a favourable count of 10π electrons. This interplay of unfavourable N_{55} and favourable N_{57} has been proposed as a rationale for the favouring of the one-heptagon cage [12, 13]. Consideration of edge types therefore goes some way to explaining the features of the low-energy isomers, although it does not yet give a clear understanding of what the six disparate cages in Figure 1 have in common.

HOMO-LUMO gap

In independent-electron models, the HOMO-LUMO gap of a molecule has a direct correlation with reactivity, susceptibility to electron loss or electron gain, and overall chemical stability. For fullerenes and polycyclic aromatic hydrocarbons, in particular, HOMO-LUMO gap weighted by the number of conjugated atoms [27], or divided by that of a reference system [28], have been proposed as measure of kinetic stability. Table 1 shows that the widest HOMO-LUMO gaps amongst the considered isomers of C_{58} are 2.22, 1.96 and 1.96 eV, but that the corresponding isomers are not those of lowest energy. However, for C_{60}, the widest HOMO-LUMO gaps are 2.76, 2.00 and 2.00 eV, in rough agreement with the order of relative energies. For C_{62}, widest gaps correspond to C_{62}-4-8, C_{62}^{1s}-2-23 and C_{62}^{1s}-1-1, also in poor agreement with the energy order. Overall, the HOMO-LUMO gaps would be taken to imply that isomers with a single square face have more favourable energies than classical fullerenes, or fullerenes with a single heptagon, whereas the opposite is in fact the case. Calculation of gaps is in any case problematic with DFT methods, but it is clear that HOMO-LUMO gap is an imperfect indicator for thermodynamic stability of fullerenes.

Asphericity

The asphericity parameter (AS) is a value that characterizes a global geometrical feature of a cage-shaped molecule. A 'rounder' fullerene isomer has a smaller AS value, and could be expected on purely steric grounds to be more stable than the other isomers since it has a smaller average departure from ideal sp^2 hybridization geometry [29]. The index is defined in terms of mean square derivation from average cage radius as [30]:

$$AS = \sum_i \frac{(r_i - r_0)^2}{r_0^2}$$

Where r_i is the distance between atom i and the cage centre of gravity, and r_0 is the average of these distances. AS values were calculated for all isomers optimized at the DFT/6-31G* level.

For C_{58}, the three most favoured isomers are not those of smallest AS, and it appears that AS is a good indicator of stability only within the classical isomers of equal N_{55}. For C_{60}, the three isomers of lowest energy (all classical) have the smallest AS values, but the non-classical isomers do not follow a rule of minimization of AS, even for equal numbers of pentagon adjacencies. For C_{62}, the three most favoured isomers do not have smallest values of AS and again only the classical isomers of equal N_{55} obey a minimization rule. In a word, asphericity may be a useful ancillary indicator of stability of classical fullerenes with a fixed number of pentagon adjacencies, but it clearly does not cope with the structural variety of the square- and heptagon-containing cages.

Pyramidalisation angles

Fullerenes are formally composed of sp^2 carbon centres for which the ideal local geometry is planar. As Haddon has pointed out [31], the existence of non-hexagonal faces in a classical fullerene has an implication for the hybridisation of the carbon centres. Given the directions of the three edges meeting at a vertex, the direction of the remaining pπ orbital axis vector (POAV), and hence the pyramidalisation angle, can be calculated. These calculations were made here for all atoms of the optimized cages. The values obtained are not very different from those calculated purely combinatorially by assuming that the three local faces are regular polygons: the nominal values for vertex types encountered in classical and non-classical fullerenes are (466) 18.4º, (555)

20.9º, (556) 16.7º, (557) 13.1º, (566) 11.6º, (567) 6.3º, (666) 0, (667) -9.5º. The same trend is almost exactly reproduced by the combinatorial curvature calculated from the mathematical expression [32]

$$\varphi(i) = 1 - \frac{1}{2} d_i + \sum_{j=1}^{d_i} \frac{1}{f_{ij}}$$

Where d_i is the degree of vertex i and the $f_{i,j}$ are the sizes of the d_i faces (j = 1, … d_i) incident at that vertex. This expression gives curvatures (466) 1/12; (555) 1/10; (556) 1/15; (557) 3/70; (566) 1/30; (567) 1/105; (666) 0; (667) -1/42.

Changing the angle sum from 360º at an sp^2 carbon weakens π bonding through loss of overlap and also leads to σ strain as the individual angles deviate from the 120º ideal. We use the average of the POAV angle within each of the six vertex types as a possible index of influence on the stability. These averages follow the combinational order: $V_{466}>V_{556}>V_{557}>V_{566}>V_{567}>V_{666}$. This order rationalizes both the unfavourable effect of the square, and the favourable effect of pentagon-heptagon fusion. However, by the same token, the POAV viewpoint cannot account for the low energy of square-containing $C_{62}^{1s}(C_{2V})$. Even so, the POAV measure is more successful for classical and one-heptagonal C_{62}: isomers the most favoured classical and heptagon-containing isomers of C_{62} have an equal number of fused pentagons (N_{55} = 3), but the strain in the vertices at pentagon-pentagon junctions has been partly released by the heptagonal neighbor in the latter, and thus the lower energy of the one-heptagon cage complies with POAV. This measure is both more local than asphericity, and more directly related to a purely graph-theoretical treatment of the cage as a polyhedral network of faces.

Structural nepotism

Direct inspection of the polyhedral cages suggests that the favoured cages have structural motifs in common. A large part of the fullerene framework is conserved amongst the six low-energy isomers of C_{58} to C_{60}, both within isomeric pairs and in pairs that are formally related by C_2 gain or loss. The two most stable isomers of C_n are related by single Stone-Wales transformations. These relationships are summarised in Fig. 3.

As we have seen, neither HOMO-LUMO gaps nor AS rules can rationalize the unique

stability of the non-classical fullerenes with a heptagon or square, and POAV gives only a partial account of the calculated results. Conservation of structural motifs is more successful as a criterion of stability, as shown in the present section and in agreement with recent work by other authors on classical endohedral fullerenes [33].

For isomers with a square, there are only ten pentagons, increasing the likelihood of an isomer without pentagon adjacencies. In fact, as noted earlier, some isomers with one or two squares are favoured over classical cages for C_{24} and C_{26} [18, 19]; by extension it might be expected that a favoured square-containing isomer would be more likely for C_{58} than the larger C_{62}. However, the best square-containing isomer of C_{58} is higher by 28.56 kcal/mol than the best classical cage and ranks only twelfth among all isomers, whereas the most favoured square-containing isomer of C_{62}, C_{62}^{1S}-0-1(9620), lies 10.4 kcal/mol below the best classical isomer.

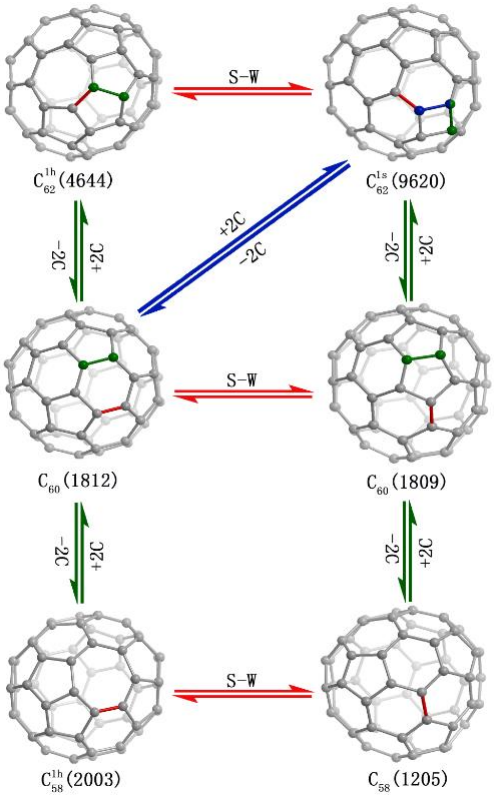

Fig.3 Structural nepotism amongst the lowest energy isomers of C_{58}, C_{60} and C_{62}. Horizontal arrows indicate single Stone-Wales rotations, and vertical and diagonal arrows indicate direct addition/extrusion of a pair of carbon atoms by the Endo-Kroto mechanism.

According to the Euler theorem, adding a heptagon will require an extra pentagon for carbon

fullerenes which is typically a disfavoured change as, by the same reasoning, it may lead to more fused pentagons in the original framework. There are 13 pentagons in the frameworks of heptagon-containing C_{58} and C_{62}. There are also at least four and three pairs of fused pentagons. However, heptagon-containing C_{58}^{1h}-4-1(2003) and C_{62}^{1h}-3-1(4644) are the second and first favoured isomers, respectively. As before, we note that increase in edges of type 57 is typically stabilising.

I_h-C_{60} is the first IPR-satisfying fullerene isomer, and in this cage all carbon atoms have identical chemical environments. Both C_{58}^{1h}-4-1(2003) and C_{62}^{1h}-3-1(4644) have 13 pentagons and four and three of the energetically unfavourable pentagon adjacencies, respectively. However, both structures can be obtained formally from I_h-C_{60} by direct removal/addition of a B_{56} bond. Of the active carbon atoms at the junctions of fused pentagons, some are shared with the heptagon, forming a local near-planar structure of edges. The pyramidalisation angles at the heptagon are significantly smaller than at carbon atoms in 556 sites and the strain at the fused pentagons is released to some extent.

Some square-containing isomers are also structurally close to I_h-C_{60}. For example, isomer C_{62}^{1S}-0-1(9620), although it contains a highly strained square, is IPR-satisfying and can be formed by adding a C_2 unit parallel to a B_{66} bond of I_h-C_{60} or C_{2v}-C_{60} as shown in Fig.3. In other words, it is equivalent to a local modification of the structure I_h-C_{60}, which is consistent with a significant retention of the favourable environment for π-bonding. The implication is that the most stable isomers, both classical and non-classical, inherit stability from their I_h-C_{60} relative.

Ring currents

The ability to sustain a diatropic ring current in the presence of an external magnetic field is often taken as an indicator of aromaticity in π-monocycles [34] and, by extension, in polycycles and 3D structures. *Ab initio* calculation of current-density maps using the ipsocentric approach [35-37] is well established and economical but can still be costly for large systems. A simple expedient that reproduces the essential features of current maps for 2D molecules is the pseudo-π method [22], in which the carbon centres of a conjugated system are formally replaced by hydrogen centres (represented by an STO-3G 1s orbital, with idealized C-C distances of 1.4 Å), thus converting a π system into a σ analogue. This σ/π analogy broadly carries over to 3D systems

[23]. In our maps, diatropic ('aromatic') ring currents are conventionally represented by anticlockwise, and paratropic ('antiaromatic') by clockwise circulations.

In polyhedral systems, such as the fullerenes, there are two standard choices for representation of magnetic response: we can take a single direction of the external field and superimpose the response of multiple layers of atoms (as in the stack-of-plates model [38]), or we can take each face and apply a radially directed field to find the local ring current per face. The second choice, which highlights 'potential aromaticity' of each face of the fullerene, is adopted here. When applied to I_h-C_{60} [23], the pseudo-π method gives a pattern that is similar to the results from all previous calculations, with essentially localised circulations in neighbouring hexagons being driven by the paratropic pentagons. Calculations at the empirical Hückel-London (HL) level [39, 40] also showed strong paratropic currents in the pentagonal rings, and diatropic currents that are weaker (by an order of magnitude) in the hexagons. Full *ab initio* calculation of all-electron current at the Hartree-Fock [41] and density-functional [42] levels show the same qualitative picture for current on the exterior of the carbon sphere; the DFT calculations additionally suggest a reversal of current deep on the interior 'face' of the sphere. Significant cancellation of contributions to magnetisability may arise from the different ring types [40], from different interior and exterior behaviour [42], and presumably from different orientations of the rings with respect to external field.

Fig. 4 shows views of ring currents calculated in the pseudo-π approach for typical structural motifs of the isomers featured in Fig. 1. The generic features of current maps for rings of different sizes are illustrated by Fig. 4. Square rings (Fig. 4(a)) support strong paratropic, and hence antiaromatic, currents. Isolated pentagons (Fig. 4(b)) have the same antiaromatic signature. Fusion of pentagons to form isolated pentalene units (Fig. 4(c)) leads to an 8π-cycle paratropic circulation, also antiaromatic. In contrast, an isolated hexagonal ring (from I_h-C_{60}), (Fig. 4(d)), supports no global ring current at all: the map shows three components that might appear to be parts of a diatropic ring current, but the breaks in connection indicate that these are actually parts of paratropic circulations in neighbouring (pentagonal) rings. This local pattern in hexagons seems to be generic across the set of stable isomers.

The isomer C_{62}^{1h} -3-1(4644) is the lowest-energy form of C_{62}. It contains a heptagon

surrounded by a chain of four fused pentagons, two isolated hexagons and an isolated pentagon (see Fig. 2). The current map (Fig. 4(e)) shows an anticlockwise (diatropic) circulation in the heptagon, with concentration in the region of pentagon neighbours. In the C_{58} isomer (Fig. 4(f)), the piecewise diatropic current appears to be driven by the paratropicity of neighbouring pentagon-containing moieties. There is a clear analogy with the currents in the hexagonal faces of I_h-C_{60}.

It has been debated whether fullerenes such as C_{60} are aromatic in the normal sense (see, for example, the review in [43]). It may be that an isomer of C_{50} is the only example of a fullerene with the 'spherical aromaticity' [44] that was predicted for systems with $2(N+1)^2$ π electrons [45]. What we can say in the present context is that the local currents in the favoured isomers of the classical and non-classical isomers in the size range studied here show a strong family resemblance to those of the stable C_{60} molecule.

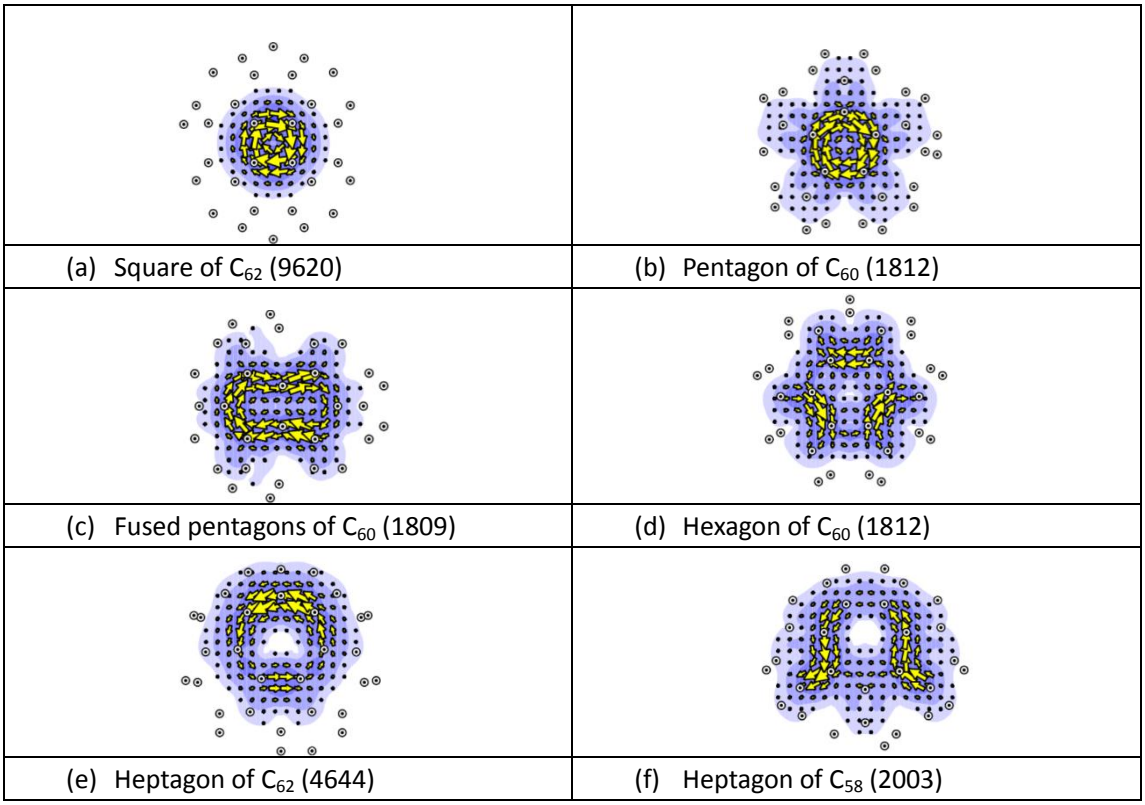

Fig.4. Ring-current maps for radial fields on selected polygonal faces of isomeric fullerenes C_{58} to C_{62}

Conclusion

A systematic DFT study of classical and non-classical isomers of C_{58}, C_{60} and C_{62} has explored questions of similarity of the stable structures in the size range. Small changes can convert good structures into bad. Geometrical motifs correlate with stability: for example, the calculations indicate that favoured one-heptagon isomers tend to have more vertices of type 557, whereas favoured one-square isomers tend to have fewer vertices of type 455. Ring-current simulations demonstrate that both squares and pentagons support paratropic (anti-aromatic) current under radial magnetic fields, whereas hexagons and heptagons tend to be localized in their magnetic response and driven by the paratropicity of neighbouring small rings. Analysis of the structures shows a tendency to 'nepotism' amongst the most favoured isomers of C_{58}, C_{60} and C_{62}, in that inheritance of favoured local motifs accounts for the special status of corresponding isomers.

Acknowledgements

Li-Hua Gan thanks the National Natural Science Foundation of China (51272216, 51472208); CMG and JC thank Sheffield University and EPSRC for support through studentships.

References

1. H. W. Kroto, J. R. Heath, S. C. O'Brien, R. F. Curl and R. E. Smalley, *Nature,* 1985, **318**, 162.

2. H. Kroto, *Nature*, 1987, **329**, 529.

3. E. Albertazzi, C. Domene, P. W. Fowler, T. Heine, G. Seifert, C. Van Alsenoy and F. Zerbetto, *Phys. Chem. Chem. Phys.*, 1999, **1**, 2913.

4. E. E. B. Campbell, P. W. Fowler, D. Mitchell and F. Zerbetto, *Chem. Phys. Lett*., 1996, **250**, 544.

5. S. Díaz Tendero, F. Martín and M. Alcamí, *ChemPhysChem*, 2005, **6**, 92.

6. P. D. W. Boyd and C. A. Reed, *Acc. Chem. Res.*, 2005, **38**, 235.

7. V. Georgakilas, J. A. Perman, J. Tucek and R. Zboril, *Chem. Rev*., 2015, **115**, 4744.

8. Y. Z. Tan, R. T. Chen, Z. J. Liao, J. Li, F. Zhu, X. Lu, S. Y. Xie, J. Li, R. B. Huang and L. S. Zheng, *Nat. Commun.*, 2011, **2**, 420.

9. Y. Zhang, K. B. Ghiassi, Q. Deng, N. A. Samoylova, M. M. Olmstead, A. L. Balch and A. A. Popov. *Angew. Chem. Int. Ed.*, 2015, **54**, 495.

10. L. H. Gan, Dan Lei and P. W. Fowler, *J. Comput. Chem.*, 2016, **37**, 1907.

11. E. Hernandez, P. Ordejon and H. Terrones, *Phys. Rev. B*, 2001, **63**,193403.

12. L. H. Gan, J. Q. Zhao and Q. Hui, *J. Comput. Chem.*, 2010, **31**, 1715.

13. A. Ayuela, P. Fowler, D. Mitchell, R. Schmidt, G. Seifert and F. Zerbetto, *J. Phys. Chem.*, 1996, **100**, 15634.

14. G. Brinkmann, O. Delgado Friedrichs, S. Lisken, A. Peeters, N. Van Cleemput, *MATCH Commun. Math. Comput. Chem.*, 2010, **63**, 533. http://www.math.uni-bielefeld.de/~CaGe

15. P. W. Fowler and D. E. Manolopoulos, An Atlas of Fullerenes; Clarendon Press: Oxford, 1995.

16. D. E. Manolopoulos and P. W. Fowler, *Chem. Phys. Lett*., 1993, **204**, 1; P. W. Fowler, M. Jooyandeh and G. Brinkmann, *J. Math. Chem.,* 2012 **50**, 2272; G. Brinkmann, J. Goedgebeur and B. D. McKay, *Chem. Phys. Lett.,* 2012, **522**, 54.

17. L. H. Gan, *Chem. Phys. Lett*., 2006, **421**,305.

18. J. An, L. H. Gan, J. Q. Zhao and R. Li, *J. Chem. Phys*., 2010, **132**, 154304.

19. W. An, N. Shao, S. Bulusu and X. C. Zeng, *J. Chem. Phys*., 2008, **128**, 084301.

20. P. W. Fowler, D. Mitchell, G. Seifert and F. Zerbetto, *Fullerene Science and Technology*, 1997, **5**, 747.

21. M. J. Frisch, et al, Gaussian 09, Revision D.01, Gaussian, Inc., Wallingford CT, 2009.

22. P. W. Fowler and E. Steiner, *Chem. Phys. Lett*., 2002, **364**, 259.

23. A. Soncini, R.G. Viglione, R. Zanasi, P.W. Fowler and L.W. Jenneskens, *Compte. Rendus Chimie,* 2006,**9**, 1085.

24. P. W. Fowler and W. Myrvold, *J. Phys. Chem. A,* 2011,**115**, 13191.

25. P. Lazzeretti and R.Zanasi, SYSMO Package; University of Modena: Modena, Italy, 1980. Additional routines by P. W. Fowler; E. Steiner, R. W. A. Havenith and A. Soncini.

26. Y. H. Cui, D. L. Chen, W. Q. Tian and J. K. Feng, *J. Phys. Chem. A*, 2007, **111**, 7933.

27. J. -I. Aihara, *Theor. Chem. Acc*., 1999**, 102**, 134.

28. J. -I. Aihara, *J. Phys. Chem. A*, 1999, **103**, 7487.

29. T. G. Schmalz, W. A. Seitz, D. J. Klein and G. E. Hite, *J. Am. Chem. Soc*., 1988, **110**, 1113.

30. P. W. Fowler, T. Heine and F. Zerbetto, *J. Phys. Chem. A,* 2000, **104**, 9625.

31. R. C. Haddon, *J. Phys. Chem. A*, 2001, **105**, 4164.

32. P. W. Fowler, S. Nikolić, R. D. L. Reyes and W. Myrvold, *Phys. Chem. Chem. Phys*., 2015, **17**, 23257.

33. Y. Wang, S. Díaz-Tendero, F. Martín, M. Alcamí, *J. Am. Chem. Soc.,* 2016, **138**, 1551.

34. P. R. Schleyer, C. Maerker, A. Dransfeld, H. Jiao and N. J. R. E. Hommes, *J. Am. Chem. Soc*., 1996, **118**, 6317.

35. T. A. Keith and R. F. W. Bader, *Chem. Phys. Lett.*, 1993, **210**, 223.

36. S. Coriani, P. Lazzeretti, M. Malagoli and R. Zanasi, *Theor Chim Acta*, 1994, **89**, 181.

37. E. Steiner and P. W. Fowler, *J. Phys. Chem. A*, 2001, **105**, 9553.

38. P. W. Fowler and A. Soncini, Phys. *Chem. Chem. Phys.*, 2011, **13**, 20637.

39. V. Elser and R. C. Haddon, *Nature*, 1987, **325**, 792.

40. A. Pasquarello, M. Schlüter and R. C. Haddon, *Science*, 1992, **257**, 1660.

41. R. Zanasi, P. Lazzeretti and P. W. Fowler, *Chem. Phys. Lett.,* 1997, **278**, 251.

42. M. P. Johansson, J. Jusélius and D. Sundholm, *Angew. Chem. Int. Ed*. 2005, **44**, 1843.

43. J. A. N. F. Gomes and R. B. Mallion, *Chem. Rev.,* 2001, **101**, 1349. (See section VIII.)

44. A. Sanz Matías, R. W. A. Havenith, M. Alcamí and A. Ceulemans, *Phys. Chem. Chem. Phys*., 2016, **18**, 11653.

45. A. Hirsch, Z. Chen and H. Jiao, *Angew. Chem., Int. Ed*., 2000, **39**, 3915.